Radio Jets in Galaxies with Actively Accreting Black Holes: new insights from the SDSS

Guinevere Kauffmann[1], Timothy M. Heckman[2], Philip N. Best[3]

[1]*Max-Planck Institut für Astrophysik, D-85748 Garching, Germany*
[2]*Department of Physics and Astronomy, Johns Hopkins University, Baltimore, MD 21218*
[3]*Institute for Astronomy, Royal Observatory Edinburgh, Blackford Hill, Edinburgh EH9 3HJ, Scotland, UK*

Abstract

In the local Universe, the majority of radio-loud AGN are found in massive elliptical galaxies with old stellar populations and weak or undetected emission lines. At high redshifts, however, almost all known radio AGN have strong emission lines. This paper focuses on a subset of radio AGN with emission lines (EL-RAGN) selected from the Sloan Digital Sky Survey. We explore the hypothesis that these objects are local analogs of powerful high-redshift radio galaxies. The probability for a nearby radio AGN to have emission lines is a strongly decreasing function of galaxy mass and velocity dispersion and an increasing function of radio luminosity above 10^{25} W Hz^{-1}. Emission line and radio luminosities are correlated, but with large dispersion. At a given radio power, radio galaxies with small black holes have higher [OIII] luminosities (which we interpret as higher accretion rates) than radio galaxies with big black holes. However, if we scale the emission line and radio luminosities by the black hole mass, we find a correlation between normalized radio power and accretion rate in Eddington units that is independent of black hole mass. There is also a clear correlation between normalized radio power and the age of the stellar population in the galaxy. Present-day EL-RAGN with the highest normalized radio powers are confined to galaxies with small black holes. High-redshift, high radio-luminosity AGN would be explained if big black holes were similarly active at earlier cosmic epochs.

To investigate why only a small fraction of emission line AGN become radio loud, we create matched samples of radio-loud and radio-quiet AGN and compare their host galaxy properties and environments. The main difference lies in their environments; our local density estimates are a factor 2 larger around the radio-loud AGN. We propose a scenario in which radio-loud AGN with emission lines are located in galaxies where accretion of both cold and hot gas can occur simultaneously. At the present day, these conditions are only satisfied for low mass galaxies in dense environments, but they are likely to apply to most galaxies with massive black holes at higher redshifts.

1 Introduction

Over the last few years, there has been growing realization that the powerful relativistic jets associated with radio galaxies may play a very important role in regulating the star formation histories of the most massive galaxies in the Universe. X-ray studies of groups and clusters of galaxies with *Chandra* and *XMM-Newton* have shown that these jets interact strongly with their environment, blowing clear cavities or "bubbles" in the surrounding X-ray emitting gas (Böhringer et al. 1993; Fabian et al. 2000,2003,2005; Churazov et al. 2001; Birzan et al. 2004; Forman et al. 2005). Studies of the demographics of nearby radio galaxies show that the jet phenomenon is primarily associated with the most massive galaxies and black holes in the local Universe (Best et al 2005b; hereafter B05b). Radio galaxies are also found to be preferentially located in central group and cluster galaxies when compared to other galaxies of the same mass (Best et al 2007). Gas cooling rates are expected to be the highest in these systems, but it can be shown that the integrated energy input by radio jets is likely to be sufficient to shut off the cooling and star formation in these massive galaxies, leading naturally to the observed exponential cutoff at the bright end of the galaxy luminosity function (B05b; Best et al 2006; Croton et al 2006; Allen et al 2006).

It has long been known that radio galaxies can be divided into two major classes (Fanaroff & Riley 1974). In Class I (FRI) sources, the radio emission peaks near the center of the galaxy and the emission from the jets fades with distance from the center. Class II (FRII) sources have "edge-brightened" radio lobes. Class I sources dominate at low radio power and low redshifts, while high power radio galaxies with 178MHz radio powers greater than 10^{27} W Hz^{-1} are almost exclusively FRII systems. Another way of classifying radio galaxies is according to whether they have strong high-excitation narrow-line emission. The objects lacking emission lines are sometimes referred to as low-excitation radio galaxies (Hardcastle, Evans & Croston 2006). The majority of low-power, FRI radio galaxies are low excitation systems. Conversely, most powerful, high-redshift FRII radio galaxies have strong emission lines.

In the local Universe, the majority of radio galaxies are relatively low power FRI radio sources. They are found in typical elliptical galaxies with very little ongoing star formation and weak emission lines (Ledlow & Owen 1995; Govoni et al 2000; B05b). If optical emission lines are present, they generally have s LINER-type line ratios. X-ray studies of low-excitation radio galaxies are consistent with a model in which the active nuclei of these objects are not radiatively efficient in any waveband (Hardcastle, Evans & Croston 2006). There is almost never any evidence of a heavily absorbed nuclear X-ray component, which suggests that a classical accretion disk and obscuring torus is not present in these systems. Recently Allen et al (2006) have shown that a tight correlation exists between the Bondi accretion rates calculated from the observed gas temperature and density profiles and estimated black hole masses, and the power emerging from these systems in relativistic jets. This result suggests that the jets are being powered by accretion from hot gas halos surrounding the galaxy.

In the nearby Universe, powerful FRII radio galaxies have much lower volume densities compared to the FRIs, but the FRII space density appears to increase very strongly as a function of redshift (Laing, Riley & Longair 1983; Dunlop & Peacock 1990). It has been established that powerful FRIIs exhibit a strong correlation between their radio and their emission line luminosities (Baum, Zirbel, O'Dea 1995). This suggests that both the optical and the radio emission are linked to the same physical process. It is also generally accepted that powerful FRII radio galaxies and radio-loud quasars are likely to be the same objects, observed at different viewing angles to the axis of the jet (Barthel 1989). As such, the black holes in powerful FRIIs are undergoing *radiatively efficient* accretion and the optical line emission is likely powered by gas from an accretion disk.

It should be noted that although there is a gross connection between Fanaroff-Riley class and the presence or absence of emission lines, the relation is certainly not one-to-one. A significant number of reasonably powerful FRII radio galaxies are in fact low excitation systems (Hine & Longair 1979; Laing et al 1994; Hardcastle et al 2006). This indicates that the transition between FRI and FRII radio morphology and that between radiatively efficient and inefficient accretion are different phenomena, even though both occur at similar radio luminosities. The physical origins of this difference are not understood.

Understanding the circumstances under which an accreting black hole is able to produce a radio-jet is extremely important if we wish to understand how AGN feedback can affect galaxies at different redshifts. In current theoretical models, feedback from radio AGN is only assumed to play an important role for massive black holes located at the centers of dark matter halos that contain a substantial reservoir of hot X-ray emitting gas (Croton et al 2006; Bower et al 2006; Sijacki et al 2007). At high redshifts, massive X-ray emitting halos are rare and it has been postulated that large-scale outflows from quasars become more important in regulating the growth of the most massive galaxies (Di Matteo, Springel & Hernquist 2005; Hopkins et al 2005). The FRII radio galaxy phenomenon has largely been neglected up to now.

Ideally, one would like to carry out a controlled comparison of different classes of radio-loud and radio-quiet AGN in order to address some of the issues discussed above. It is important that different AGN classes be compared at the same redshift, so that evolutionary effects do not complicate the analysis. Recently, B05b compared the host galaxy properties of radio-loud AGN with those of optically- selected narrow-emission line AGN. Both samples were drawn from the main spectroscopic sample of the Sloan Digital Sky Survey. As mentioned previously, the sample of radio galaxies analyzed by B05b was dominated by very massive early-type galaxies with weak or undetectable optical emission lines. A minority of radio galaxies with emission lines can be found in this sample, however, and it is these objects which are the focus of the analysis in the present paper. We use our sample of radio galaxies with emission lines to address the following questions:

1. Is there a correlation between radio luminosity and emission line luminosity for these low redshift systems? If so, how does this compare with results in the literature, which have generally included radio galaxies at higher redshifts than those in our sample?

2. How do the host galaxies of radio AGN with emission lines compare with those of radio galaxies without emission lines?

3. How do the host galaxy and environments of radio AGN with emission lines compare with those of radio-quiet emission line AGN?

4. Do these comparisons shed any light on why some AGN develop radio jets? Can we make a link between the optical and radio AGN phenomena and different gas accretion modes as has been proposed in a recent paper by Hardcastle, Evans & Croston (2007)?

5. Can we find any evidence that feedback from the radio AGN influences the star formation histories and/or structural properties of the host galaxies of these systems?

Our paper is organized as follows. In section 2, we review how the radio galaxies in our sample were selected and describe how we differentiate between star-forming galaxies and radio AGN with emission lines. In section 3, we study the demographics of the radio galaxies with emission lines and the correlations between their radio and emission line properties. In section 4, we compare the host galaxy properties and environments of radio-loud AGN with emission lines to those of

matched samples of radio-quiet AGN. In sections 5 and 6, we compare the host galaxy properties and environments of radio-loud AGN to those of matched samples of galaxies that are selected without regard to their AGN properties and we ask whether there is any evidence that the presence or absence of a radio jet has an influence on the recent star formation history of the galaxy. Our conclusions are presented in section 7.

2 The Sample

2.1 Selection of radio-loud AGN

Best et al (2005a; hereafter B05a) identified radio-emitting galaxies within the main spectroscopic sample of the SDSS data release 2 (DR2) by cross-comparing these galaxies with a combination of the National Radio Astronomy Observatory (NRAO) Very Large Array (VLA) Sky Survey (NVSS; Condon et al. 1998) and the Faint Images of the Radio Sky at Twenty centimeters (FIRST) survey (Becker et al. 1995). The combination of these two radio surveys allowed a radio sample to be constructed that was both reasonably complete ($\sim$95%) and highly reliable (i.e. it is estimated that $\sim$99% of the sources in the catalogue are genuine radio galaxies rather than false matches). In this paper, we make use of an updated catalogue of radio galaxies based on the SDSS data release 4 (DR4).

Once the radio and optical catalogues have been cross-compared, the next task is to separate radio AGN from galaxies in which the radio emission comes primarily from star-forming regions in the galaxy. The ideal would be to identify radio AGN as those galaxies with radio flux densities that are significantly in excess of that predicted using the far-infrared/radio correlation for star-forming galaxies (e.g. Yun, Reddy & Condon 2001). However, sufficiently deep IR data were not available for this to be a viable method for the SDSS sample, so B05a separated the two populations using the location of the galaxy in the plane of 4000 Å break strength (D_n4000) versus radio luminosity per unit stellar mass. The division between star forming galaxies and AGN was motivated using Bruzual & Charlot (2003) stellar population synthesis predictions for how galaxies with different star formation histories populate this plane. The nominal dividing line was chosen to lie 0.225 in $D_n(4000)$ above the curve defined by galaxies undergoing exponentially declining star formation with a time constant $\tau = 3$ Gyr (see Fig. 9 of B05a).

One problem with the B05a criterion is that all galaxies with $D_n(4000)$ values less than 1.3 will be excluded from the radio AGN sample, regardless of their radio luminosity. In this paper, we present an alternative way of separating radio AGN from star-forming galaxies. The method is based on the correlation between radio luminosity and "corrected" Hα luminosity plotted in Figure 1 . The Hα luminosty has been corrected for dust extinction using the measured Balmer decrement [1], and for fibre aperture effects. To correct for the aperture effect, we simply scale the measured Hα luminosity by the ratio of the galaxy's Petrosian magnitude to its fibre magnitude measured in the r-band. This is only a crude correction, but as can be seen from the left-hand panel of Figure 1, galaxies classified as star-forming using the standard [OIII]/Hβ versus [NII]/Hα Baldwin, Phillips & Terlevich (1981; hereafter BPT) diagram, define a rather tight correlation in the $\log P / \log L(H\alpha)$ plane [2]. Almost all the outliers have NVSS fluxes larger than 5 mJy and are probably radio AGN. We use this tight correlation to define an AGN/SF separation line in this diagram (the dashed line).

[1] Note that in this paper, we correct emission lines such as Hα and [OIII] for extinction using the Balmer decrement, assuming a dust-free value of $H\alpha$/Hβ of 2.86 and an extinction curve of the form $\lambda^{-0.7}$ (Charlot & Fall 2000).

[2] See Kauffmann et al (2003b) for details about how galaxies are classified as star-forming or as AGN using the BPT diagnostic diagrams.

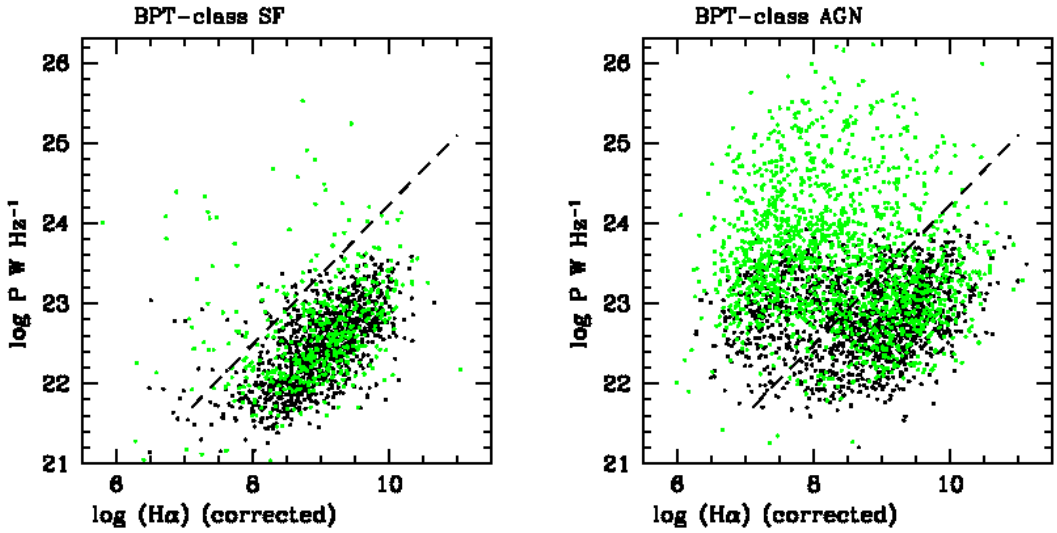

Figure 1: Separation of radio AGN and star forming-galaxies in $\log P$– $\log L(H\alpha)$ space. The left panel shows galaxies classified as star-forming from their emission line ratios using the BPT diagram diagnostic, while the right panel shows galaxies classified as optical AGN. Black points show galaxies with S(NVSS) $>$ 2.5 mJy. Galaxies with S(NVSS)$>$ 5 mJy have been overplotted using green. The dashed line is our proposed separation line for distinguishing radio AGN from galaxies where the radio emission is coming from star-forming regions. Note that L(Hα) is given in solar units and the NVSS fluxes are measured at 1.4 GHz.

We can test the robustness of our method by checking whether there is internal consistency between dividing lines that are based on different star formation indicators. Figure 2 shows radio AGN and star-forming galaxies selected using the $\log P$–$\log L(H\alpha)$ separator defined in Figure 1. We plot the location of these objects in the plane of D_n4000 versus $\log P/M_*$. As can be seen, radio AGN and star-forming galaxies segregate extremely cleanly in $D_n(4000)$–$\log P/M_*$ space. This proves that both diagrams can be used interchangeably. The dividing line in $D_n(4000)$ versus $\log P/M_*$ space that we find is slightly different to the cut proposed by B05a, which is shown as a dashed line on the plot. Nevertheless our test indicates that the method is *in principle* quite clean.

2.2 Galaxy properties from the optical spectra

A variety of physical properties have been derived for galaxies in the spectroscopic database via stellar population synthesis fitting and are publically available [3]. The stellar continuum of each galaxy is modelled as a sum of template spectra generated from population synthesis models (Tremonti et al 2004). These fits also lead to measures of stellar mass-to-light ratios, star formation histories and mean stellar ages (Kauffmann et al 2003a). After subtracting the stellar continuum, emission line fluxes can be accurately measured, allowing studies of the star formation rates (Brinchmann et al 2004) and AGN properties (Kauffmann et al 2003b; Heckman et al 2004) of the galaxies in the sample.

[3] http://www.mpa-garching.mpg.de/SDSS

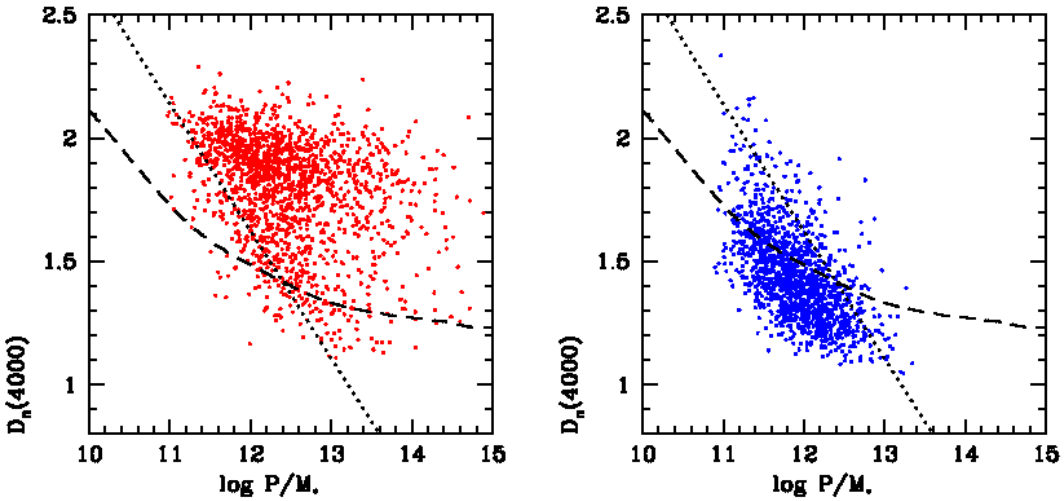

Figure 2: A consistency check of the two methods (see text). We plot $D_n(4000)$ as a function of $\log P/M_*$ for radio AGN (left) and for star-forming galaxies (right) defined using the $\log P$–$\log L(H\alpha)$ separation line plotted in Figure 1. The dashed line shows the separator defined in B05a. The dotted line has been included to guide the eye.

3 Properties of radio galaxies with emission lines

3.1 Demographics

In Figure 3, we show how the fraction of radio galaxies with emission lines depends on galaxy properties such as stellar mass, velocity dispersion and mean stellar age, as well as on radio luminosity. A radio galaxy is defined to have emission lines if the four emission lines Hα, Hβ, [OIII] and [NII] are all detected with signal-to-noise greater than 3.

In past work, we have often used the 4000 Å break index $D_n(4000)$ as an indicator of stellar age. As can be seen in Figure 3, the fraction of radio galaxies that have emission lines is a strong function of $D_n(4000)$: almost all radio galaxies with $D_n(4000)$ less than 1.6 have emission lines, and the fraction falls to below a third for $D_n(4000) > 1.8$. This result suggests that the presence of emission lines and the presence of a young stellar population in the galaxy are strongly correlated. However, low values of $D_n(4000)$ would also result if the stellar light is diluted by non-thermal AGN emission, and there has been ongoing controversy as to whether the UV continuum light from powerful radio galaxies arises from the AGN itself (either direct AGN light or light that is scattered into the line-of-sight), from young stars or from nebular continuum (see Tadhunter et al 2002 for a discussion). Therefore, to avoid any ambiguity in the interpretation of our results, we also show in Figure 3 the correlation between radio power and the Balmer absorption line Lick index Hδ_A (Worthey & Ottaviani 1997). Non-thermal light from the AGN would act to dilute the absorption lines and lower the value of Hδ_A. Any trend towards higher values of Hδ_A should be regarded as a definitive indication of the presence of young stars in the host galaxy. The top-right panel of Figure 3 demonstrates that the fraction of radio galaxies that have emission lines increases strongly with increasing Hδ_A, confirming the correlation between emission line activity and a young stellar population found in the $D_n(4000)$

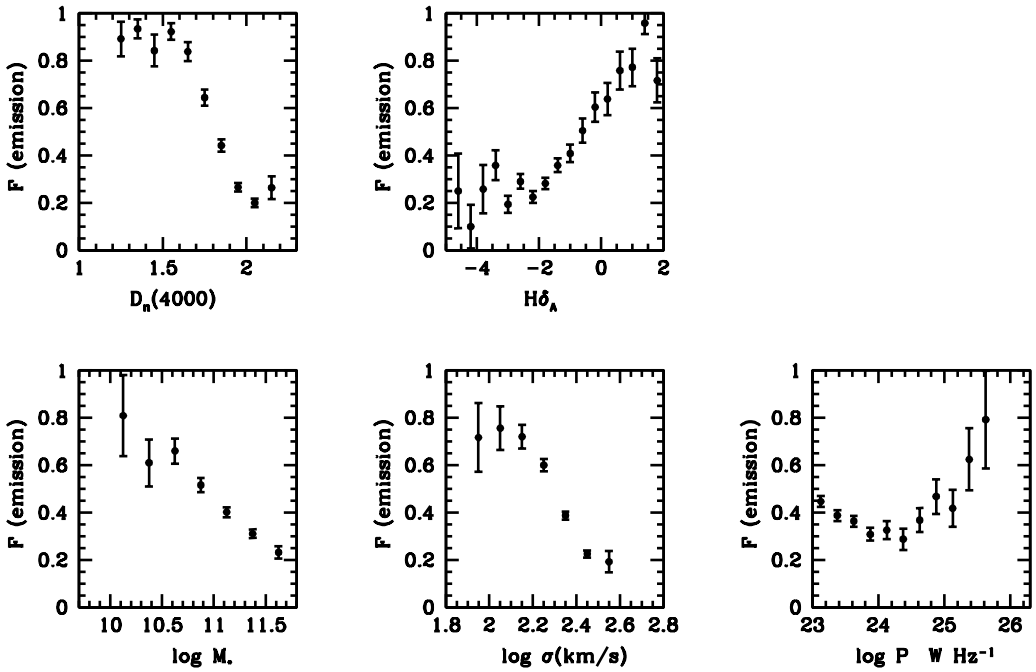

Figure 3: The fraction of radio galaxies with [OIII], Hβ, [NII] and Hα detected with $S/N > 3$ is plotted as a function of 4000 Å break, Hδ_A equivalent width, stellar mass, stellar velocity dispersion and radio power.

analysis.

The fraction of emission line radio galaxies also decreases as a function of the stellar mass and velocity dispersion of the galaxy. B05b showed that overall the fraction of radio loud galaxies is a strongly *increasing* function of both stellar and black hole mass. The results in the two bottom left panels of Figure 3 indicate that the fraction of all radio loud AGN that have emission lines has the opposite dependence on stellar mass. As a result, radio AGN with emission lines are a minority of all the radio-loud AGN in our sample (1684 out of 5714 objects with NVSS fluxes larger than 2.5 mJy).

Finally, in the bottom right panel of Figure 3, we plot the fraction of emission line radio AGN as a function of the radio luminosity. The fraction remains constant at a value of around 0.4 up to a radio luminosity of 10^{25} W Hz^{-1} and then appears to rise. It is noteworthy that this luminosity is remarkably close to the one identified by Fanaroff & Riley (1974) as the dividing point between class I and class II type sources. Fanaroff & Riley also noted that the luminosity at which the division occurs is remarkably close to that which divides sources which show strong cosmological evolution from those which do not (see also Clewley & Jarvis 2004)

3.2 Radio – emission line correlations

The question of whether the emission-line and radio luminosities of radio AGN are correlated has been examined by a number of groups. One major problem in these analyses has been the fact that the most powerful radio galaxies are always at significantly higher redshifts than the less powerful

radio galaxies in these samples. This makes it difficult to ascertain whether the primary correlation is between the emission line luminosity and radio luminosity, rather than between emission line luminosity and redshift (see McCarthy 1993 for a detailed discussion). Nevertheless, most studies have favoured the reality of the correlation (McCarthy 1993; Zirbel & Baum 1995).

We now use our sample of low-redshift radio AGN with optical emission lines to investigate this issue. B05b studied a sample dominated by radio galaxies with weak or undetected emission lines and found no overall correlation. In this section, we will focus on the subset of radio galaxies with high S/N emission lines.

As in the previous section, we consider the subsample of radio AGN with emission lines that are strong enough to allow classification on the standard BPT diagram ($S/N > 3$ in the four emission lines Hα, Hβ, [OIII] and [NII]). The luminosity the [OIII] line is corrected for extinction using the measured value of the Balmer decrement. In Figure 4, we investigate the relation between emission line and radio power for these objects. As can be seen, there is a clear correlation with substantial scatter. The absence of AGN with very high values of L[OIII] and low values of $\log P$ may, to some extent, be a selection effect. We know that very powerful AGN are usually found in galaxies with strong ongoing star formation (Kauffmann et al 2003b), so our cut on Hα luminosity (see Figure 1) may eliminate powerful optical AGN with weak radio jets. The absence of galaxies with low optical line luminosities and very high radio power is, however, a real effect.

In the right panel, we restrict the sample to high ionization optical AGN with $\log[OIII]/H\beta > 0.5$. This is the regime occupied by "pure" Seyfert galaxies where there is very little contribution from star formation to any of the emission lines (Kauffmann et al 2003b). As can be seen, although the pure Seyferts are boosted to somewhat higher [OIII] line luminosities than the sample as a whole, they exhibit much the same correlation between [OIII] line luminosity and radio luminosity. This is not surprising, since it has been demonstrated that there is very little contribution from star formation to the [OIII] line luminosity in nearby AGN (Kauffmann et al 2003b; Brinchmann et al 2004).

Interestingly, we find that a substantial part of the scatter in the relation between [OIII] line luminosity and radio power can be attributed to the spread in the masses and central velocity dispersions of the host galaxies that make up our sample. In Figure 4, we have colour-coded the points according to the value of the velocity dispersion σ measured within the fiber. Cyan points indicate galaxies with σ less than 200 km s^{-1} and red points indicate galaxies with velocity dispersions larger than this value. For a given radio power, galaxies with low velocity dispersions have higher [OIII] line luminosities on average.

We now investigate how the correlation between radio power and optical line luminosity for the low redshift SDSS radio galaxy sample compares to results obtained in past studies. Zirbel & Baum 1995; hereafter ZB) carried out the most comprehensive study of the relation between radio luminosity and emission line luminosity in radio galaxies. They concluded that FRIs and FRIIs define separate relations with differing slopes. Their data was based on narrow-band $H\alpha$ imaging, so to be consistent we now plot correlations using the total measured luminosity in the Hα and [NII] lines. In addition, we scale our results to the same assumed cosmology and radio frequency (408 MHz) used by these authors.

In Figure 5, cyan/red points show EL-RAGN with σ values lower and higher than 200 km s^{-1}, respectively. We only plot those galaxies with log [OIII]/H$\beta > 0.5$ (as shown in the right-hand panel of Figure 4), because these "high-excitation" radio galaxies are likely to be more similar to the galaxies that ZB classify as FRII sources. In addition we have supplemented the sample using radio AGN with emission lines that were too weak to allow them to be placed on the BPT diagram, but where Hα was still detected with $S/N > 3$ (Hα is usually the line with the highest S/N in the SDSS

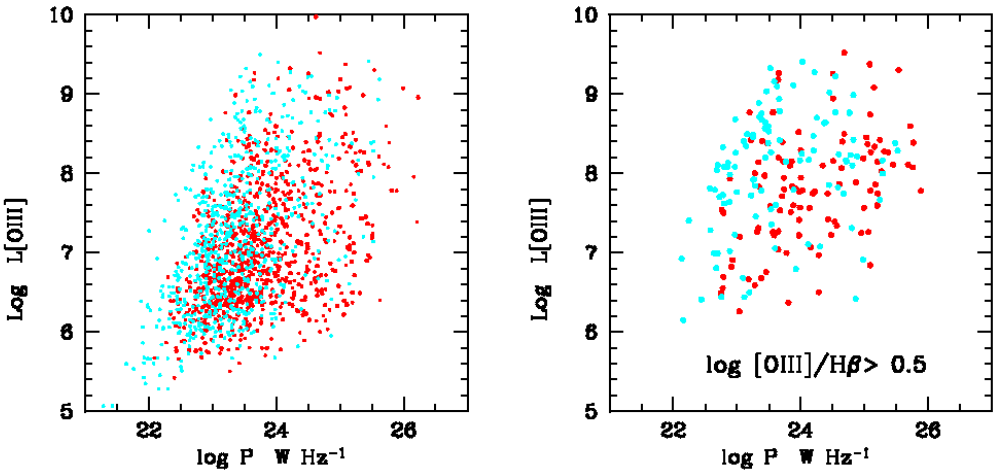

Figure 4: Left: Correlations between emission line and radio strength for the EL-RAGN sample. Cyan points indicate radio AGN with $\sigma < 200$ km/s and red points indicate radio AGN with $\sigma > 200$ km/s. Right: Results are shown for the subset of EL-RAGN with high ionization emission lines. Note that L[OIII] is in solar units. The radio luminosities are defined at 1.4 Ghz.

spectra). These galaxies are plotted as black points and they should be good analogues of the nearby FRI's studied by ZB. The vast majority of these galaxies have high central velocity dispersions. For comparison, blue crosses show radio galaxies from the sample of ZB that were classified as FRII or as "high redshift" radio sources. The dashed line shows the $L(H\alpha)$ – $\log P$ relation obtained by ZB for FRII radio galaxies, while the dotted line shows their FRI relation.

It is reassuring that the results for our weak emission-line radio AGN agree very nicely with those obtained for the ZB FRI radio galaxies. We find that our weak emission-line AGN span the same range in radio luminosities and exhibit the same correlation between radio luminosity and emission-line luminosity found by these authors. Our stronger emission-line radio AGN appear to lie on the low-luminosity extrapolation of the ZB relation for FRII galaxies. It is also worth noting that radio galaxies with high values of σ appear to lie close to a *direct* extrapolation of this relation, whereas local radio galaxies with low values of σ are offset to lower values of $\log P$. The results suggest that the more powerful FRII radio galaxies may arise when galaxies with high mass black holes accrete at a significant rate. Such systems are very rare in the low redshift Universe, but become increasingly more common at earlier epochs.

We have shown that for nearby radio AGN, the relation between emission line luminosity and radio luminosity depends on the velocity dispersion of the galaxy. In order to gain some physical understanding of this trend, we scale both the radio and the [OIII] luminosities of the AGN in our sample by dividing by the "black hole mass", which can be estimated from σ using the relation given in Tremaine et al (2002). As discussed in Heckman et al (2004), L[OIII]/M_{BH} may be regarded as a measure of the accretion rate onto the black hole in Eddington units, and measures how rapidly black holes have been building up their present-day mass. Heckman et al used this indicator to demonstrate that galaxies with low values of σ (and hence low mass black holes) are currently building up their black holes at a much higher rate in comparison to galaxies with high values of σ.

In the right hand panel of Figure 6, we plot the relation between the scaled [OIII] and radio

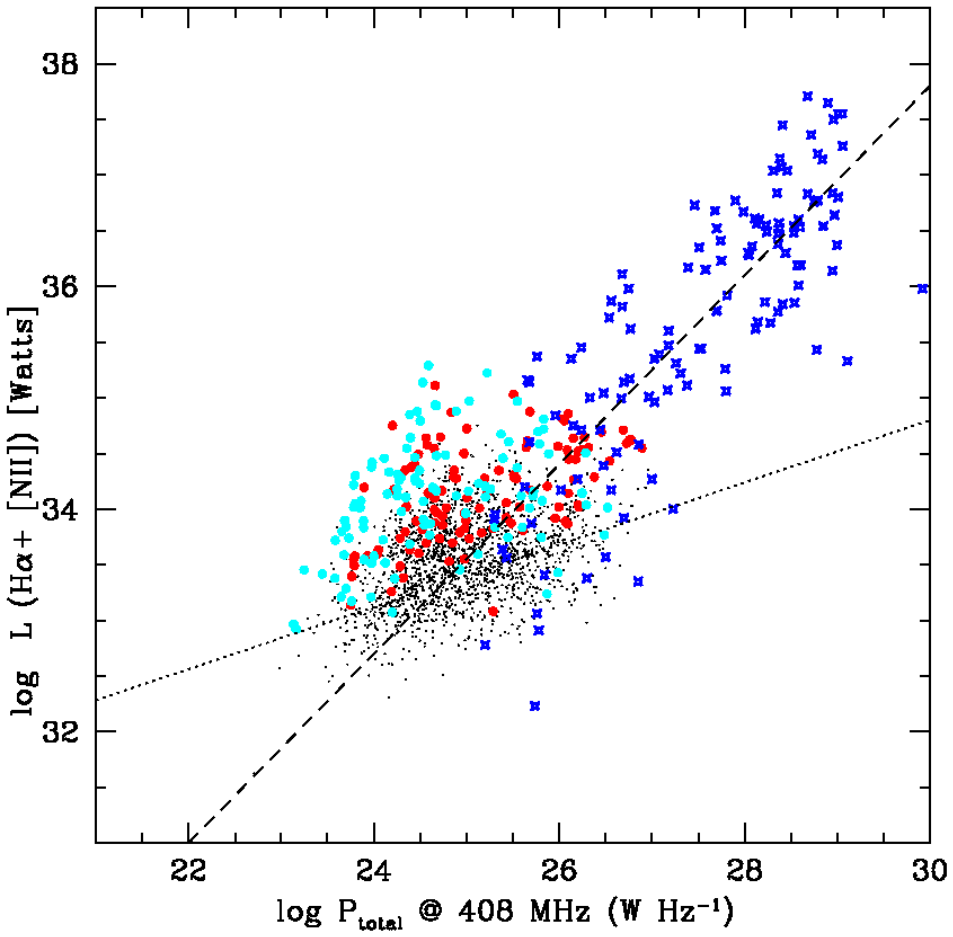

Figure 5: Comparison between our results and those of Zirbel & Baum. The sum of the Hα and [NII] emission line luminosities is plotted as a function of radio luminosity. Results have been scaled to a cosmology with $H_0 = 50$ km s $^{-1}$ Mpc^{-1} and to radio luminosities measured at 408 MHz (see text). Cyan and red points are the sample of low-σ and high-σ EL-RAGN plotted in the right-hand panel of Figure 4 (i.e. they are "high-excitation" sources with $\log[OIII]/H\beta > 0.5$) . Black points are radio AGN where Hα+ [NII] is detected with $S/N > 3$, but other emission lines are too weak to allow the galaxy to be classified on the BPT diagram. FRII and high-redshift radio galaxies from the sample of Zirbel & Baum (1995) are plotted as blue crosses. The dashed and dotted lines indicate the Zirbel & Baum fits to the FRII and FRI radio galaxies in their sample.

luminosities. As before, emission-line AGN with $\sigma < 200$ km s^{-1} are plotted as cyan points and AGN with $\sigma > 200$ km s^{-1} are plotted in red. We again find a clear correlation between the scaled quantities with substantial scatter. In agreement with results of Heckman et al (2004), there is an offset in scaled [OIII] luminosity between AGN with high/low values of σ. Interestingly, however, the offset in radio luminosity disappears after it is scaled by the black hole mass. This result is shown more quantitatively in Figure 7, where we plot the median, lower 25th percentile and upper 75th percentile of the radio luminosity at a given value of L[OIII] (left panel) and of the scaled radio luminosity at a given value of of L[OIII]/$M_{\rm BH}$ (right panel). In contrast to Figure 6, results are shown only for the RL-AGN sample. Cyan and red lines indicate galaxies with $\sigma < 200$ km s^{-1} and $\sigma > 200$ km s^{-1}, respectively. The correlation between normalized radio power and the accretion rate in Eddington units is nearly independent of black hole mass. However, the high mass (low mass) black holes dominate the distribution at low (high) normalized luminosities and accretion rates.

For completeness and to compare with the results of B05b, we also plot radio AGN without high S/N emission lines as black points in Figure 6. The L[OIII] values correspond to upper limits in the cases where the [OIII] line was not detected, or was detected with marginal significance. As can be seen, radio AGN with weak emission lines are most numerous at all but the very highest radio luminosities. The yellow dashed line indicates the median value of L[OIII] as a function of radio luminosity for the whole sample. There is essentially no trend in the median [OIII] luminosity of the radio AGN up to a radio luminosity of 10^{25} W Hz^{-1}, where there is a slight upturn (see also B05b). This upturn is considerably more pronounced if the scaled radio luminosity is used. Radio AGN with weak emission lines are absent above a scaled radio luminosity of 10^{17} W Hz^{-1} M$_{\odot}^{-1}$. In the local Universe, most such objects have low black hole masses and thus do not have extremely high total radio luminosities. At high redshifts, however, we speculate that high mass black holes will be actively accreting and typical total radio luminosities will thus be orders of magnitude higher than in our SDSS sample.

Finally, we study whether there is a correlation between radio power and the stellar populations of the radio AGN in our sample. Figure 8 shows that there is no correlation between Hδ_A and radio luminosity, but there is a trend towards younger mean stellar ages at high values of the scaled radio luminosity $\log P/$ M$_{BH}$. The majority of the radio AGN with young stellar population have low velocity dispersions. Once again we see that the *median* value of Hδ_A is set by the large number of old systems in our sample and remains constant up to a scaled radio luminosity of $\sim 10^{17}$ W Hz^{-1} $M_{\odot}^{-1}$, where it exhibits an abrupt upturn.

3.3 Section summary

Radio-loud AGN are most likely to display emission lines in galaxies with low stellar masses and velocity dispersions, and at radio luminosities greater than 10^{25} W Hz^{-1}. The radio and emission line luminosities are correlated, but with substantial scatter. At a fixed radio luminosity, AGN in low velocity dispersion hosts tend to have higher [OIII] luminosities than AGN in high velocity dispersion hosts. However, if we scale the radio and [OIII] luminosities by dividing by the black hole mass estimated from our σ measurements, we find a coorelation between normalized radio luminosity and L[OIII]/M_{BH} that is independent of black hole mass. Scaling the radio luminosity by the black hole mass also uncovers a correlation between the normalized radio power and the age of the stellar population in the host galaxy.

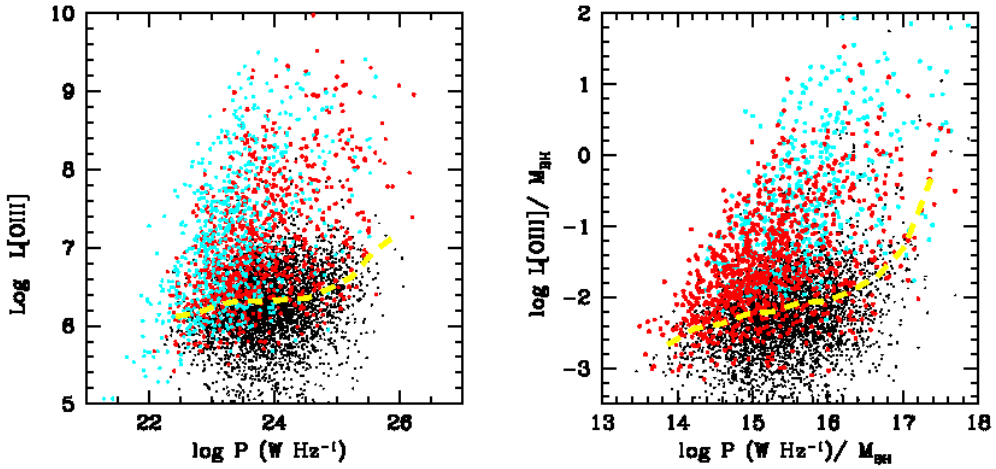

Figure 6: Correlations between emission line and radio luminosities for the full sample. Cyan points indicate radio AGN with emission lines and with $\sigma < 200$ km/s; red points indicate radio AGN with emission lines and with $\sigma > 200$ km/s; black points indicate radio AGN with weak or absent emission lines (in the case of non-detections, upper limits are plotted). In the left panel [OIII] luminosity is plotted as a function of radio luminosity. In the right panel, both the [OIII] and the radio luminosities are scaled by dividing by the black hole mass. The yellow dashed line shows the median value of L[OIII] or L[OIII]/M_{BH} as a function of radio luminosity.

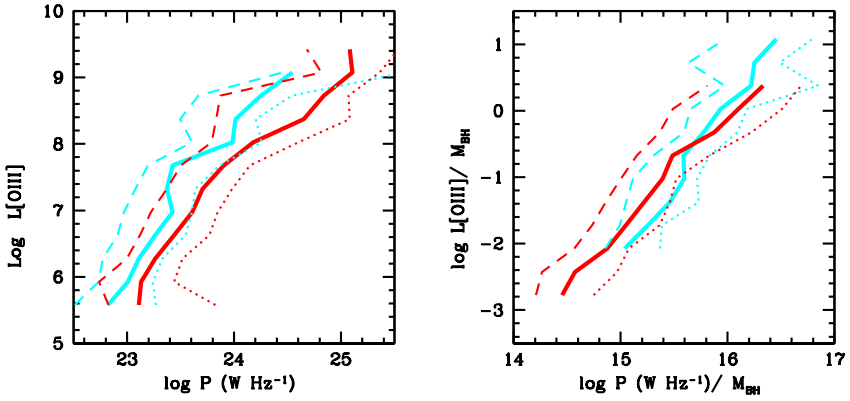

Figure 7: The figure shows the median (solid), lower 25th percentile (dashed) and upper 75th percentile (dotted) of the radio luminosity at a given value of L[OIII] (left), and the same for the scaled radio luminosity at a given value of L[OIII]/$M_{\rm BH}$ (right). In contrast to Figure 6, results are shown only for the EL-RAGN sample. The cyan curves are for galaxies with $\sigma < 200$ km s^{-1} while the red curves are for galaxies with $\sigma > 200$ km s $^{-1}$.

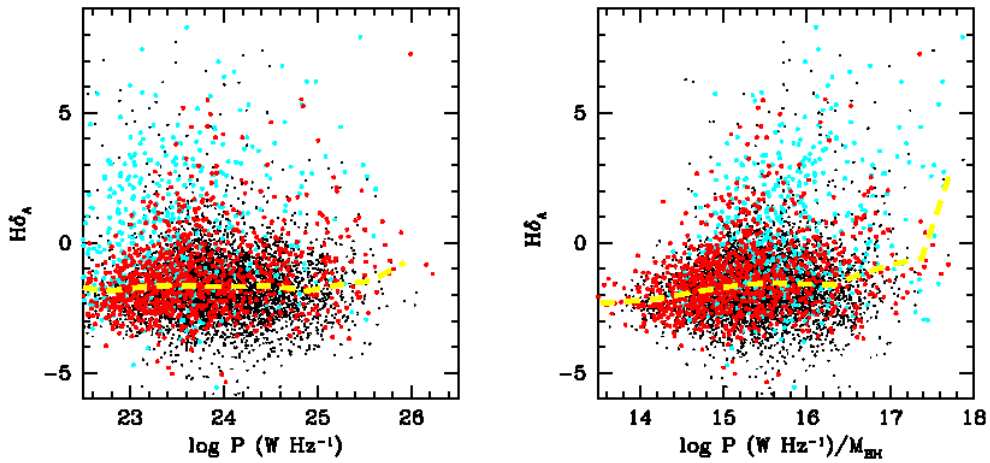

Figure 8: Correlations between Hδ_A equivalent width and radio luminosity for the full sample. The colour coding of the points is the same as in Figure 6.

4 How do radio-loud AGN with emission lines differ from radio-quiet AGN?

4.1 Host galaxies

Unlike the low excitation radio sources, which are known to occur in normal massive early-type galaxies with very little ongoing star formation, the more powerful radio galaxies with strong emission lines have been found to occupy more peculiar hosts. Smith & Heckman (1989) found that half of the powerful radio galaxies in their sample exhibited peculiar optical morphologies (tails, fans, bridges, shells and dust lanes). Their surface brightness profiles were also shallower than those of normal elliptical galaxies and many of the objects also had bluer than average colours compared to giant ellipticals. More recently, Tadhunter et al (2005) analyzed high-quality long-slit spectra for a sample of nearby powerful radio galaxies and showed that all of them had a significant young stellar component.

Care must be exercised, however, in interpreting these results as implying that the radio jet is *caused* by the same process that causes the enhanced star formation or the morphological peculiarities. Optical AGN activity has also been shown to be associated with enhanced levels of star formation in a galaxy (Kauffmann et al 2003b; Wild et al 2007). In order to disentangle the physical processes that control the radio emission from those that control the optical emission, we introduce a pair-matching technique. For each EL-RAGN, we find a radio-quiet emission line AGN (henceforth RQAGN) that is closely matched in redshift, in stellar mass and in velocity dispersion. The motivation for choosing this set of matching parameters is the following:

1. By constraining the matching galaxy to lie at the same redshift, we make sure that the fiber apertures subtend the same physical scale and that the both the radio luminosity and the optical emission line luminosity are subject to the same selection biases caused by the survey flux limits.

2. By constraining the matching galaxy to have the same velocity dispersion, we make sure that both galaxies have roughly the same black hole mass. Any AGN physics that is controlled primarily by the black hole mass will then be the same.

3. By constraining the matching galaxy to have the same stellar mass, we make sure that the host galaxies of both types of AGN are drawn from roughly similar parent galaxy populations.

Because the underlying sample of radio quiet AGN is extremely large, we have no problem imposing matching tolerances as stringent as $\Delta z < 0.01$, $\Delta \log \sigma < 0.05$ and $\Delta \log M_* < 0.1$.

Figure 9 presents a comparison of the host galaxy properties of our EL-RAGN sample (red histograms) and the matched sample of RQAGN (black histograms). The galaxy properties that we compare include the distributions of concentration, stellar surface mass density μ_*, 4000 Å break strength, Hδ absorption line equivalent width, Hα emission line equivalent width, and the "Eddington" parameter L[OIII]/M_{BH}. Note that there are around 1600 galaxies in both these samples, so the shot-noise error is small. As can be seen, the radio loud and matched radio quiet galaxies have nearly identical stellar populations and emission line properties. The property that differs the most between the two samples is the concentration index: the host galaxies of EL-RAGN appear to be slightly more concentrated than those of their radio-quiet counterparts.

4.2 Environment

We have also investigated the environments of radio-loud and radio-quiet emission line AGN. We characterize environment by computing galaxy counts down to a limiting i-band magnitude of 20.0 around each galaxy, using the SDSS photometric catalogue. The counts are evaluated as a function of angular separation out to a limiting distance of 3 arcmin. By binning together many different galaxies, we reduce the noise in this estimator. We also make a statistical correction for galaxies that are not physically associated with the AGN by computing counts around randomly distributed sky coordinates and subtracting the average uncorrelated count from our local density estimate.

Figure 10 presents results for the EL-RAGN sample. In the left panel, we plot the average number of galaxies interior to radius R . The cyan, green, red and magenta lines are for EL-RAGN binned according to increasing radio luminosity. As can be seen, the environments do not change significantly as a function of radio luminosity. This should be contrasted with the right-hand panel, in which we have binned the EL-RAGN according to velocity dispersion σ. It is clear that radio AGN with bigger bulges and black holes reside in systematically denser environments. We note that there is no trend in the median redshift of our sample of EL-RAGN as a function of radio luminosity and only a small increase in $\bar{z}$ from 0.096 for galaxies in the lowest σ bin compared to 0.132 for galaxies in the highest σ bin. Our conclusion that clustering does not depend on radio power is thus quite robust. If we were to correct for the small increase in redshift as a function of σ, this would slightly boost the environmental differences that are already quite clear from our plot.

In Figure 11, we compare the environments of the EL-RAGN with the matched sample of RQAGN. We show results in four different ranges of central velocity dispersion of σ. We find that for all values of σ, the galaxy counts around the radio-loud objects are a factor of ~ 2 higher than around their radio quiet counterparts. This is in remarkable agreement with the results of Smith & Heckman (1990) who compared the 100 kpc scale environments of a sample of 31 low redshift ($z < 0.3$) QSOs with a sample of 35 powerful radio galaxies with $\log P > 10^{25}$ W Hz^{-1}. These authors found that both the radio-loud QSOs and radio galaxies had approximately twice the average number of close companions as compared to the radio-quiet QSOs.

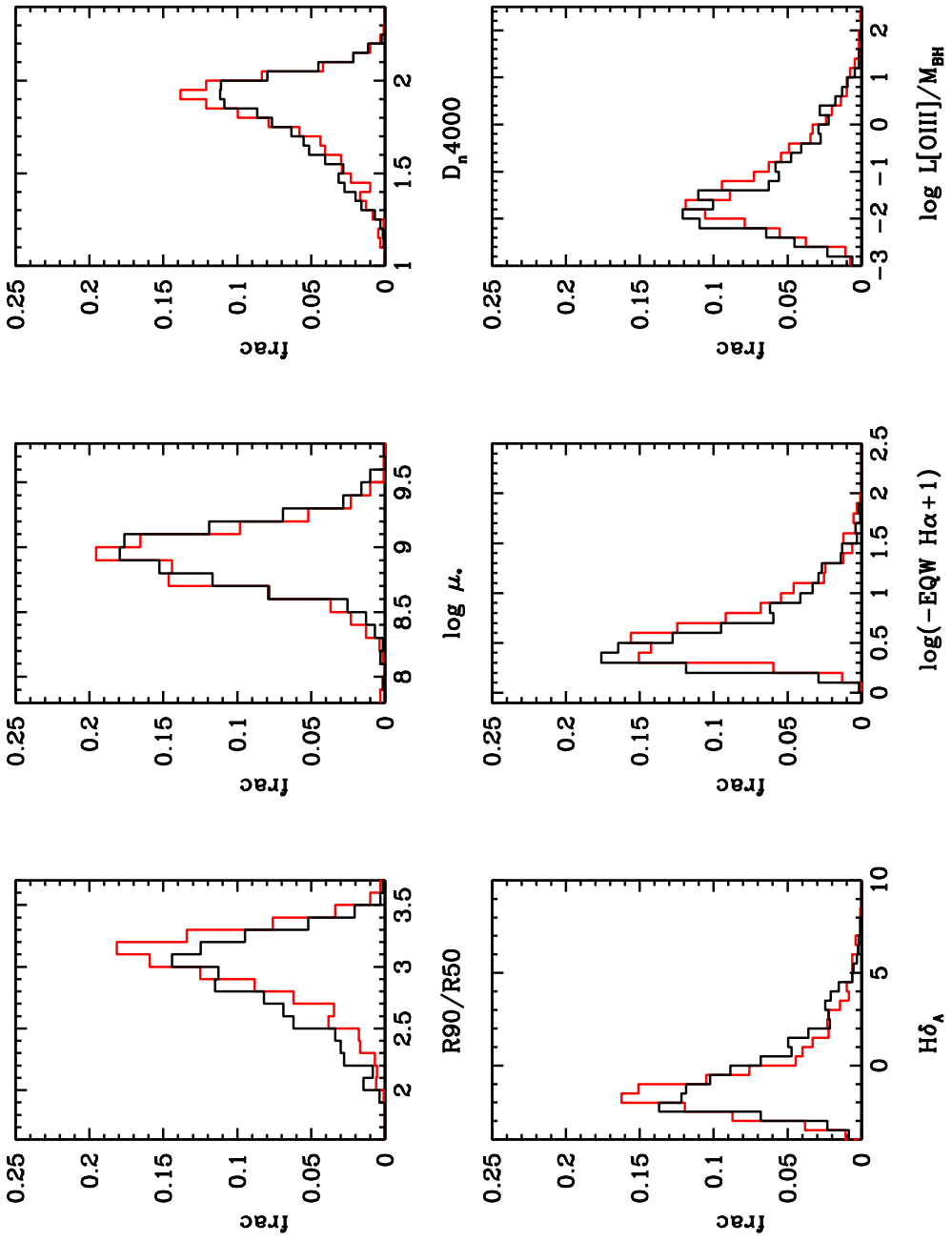

Figure 9: Comparison of host galaxy properties of EL-RAGN (red) and matched RQAGN (black). We plot histograms of concentration index (R90/R50), stellar surface mass density in units of $M_\odot$ kpc^{-2}, 4000 Å break strength, Hδ_A index, Hα equivalent width, and [OIII] luminosity normalized by black hole mass.

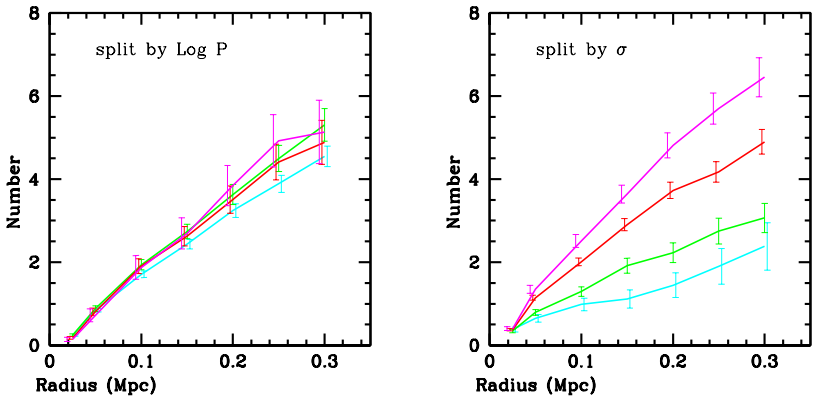

Figure 10: Galaxy counts within projected radius R in Mpc for EL-RAGN. In the left panel, the sample is split according to radio luminosity and in the right panel, the sample is split according to velocity dispersion σ. In both panels, blue, green, red and magenta lines show results for subsamples ordered in increasing radio power (left) or velocity dispersion (right).

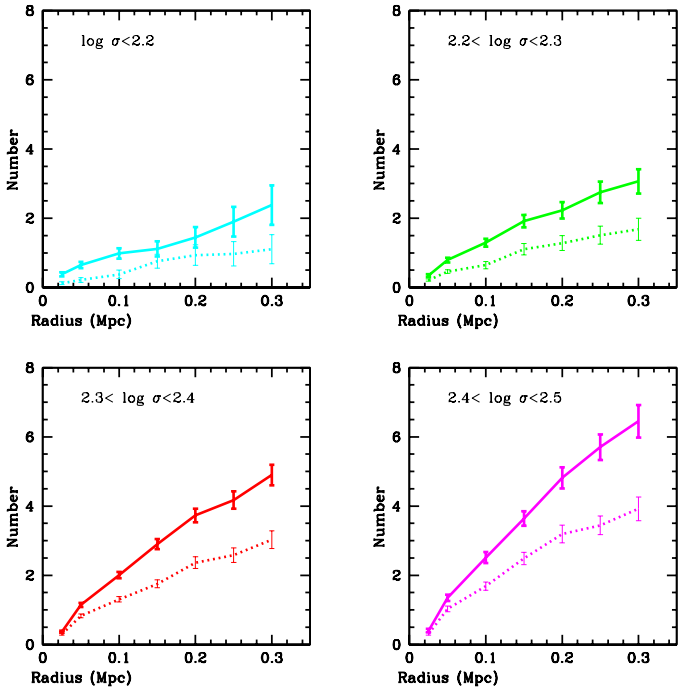

Figure 11: Galaxy counts within projected radius R in Mpc for EL-RAGN (solid) and matched samples of radio-quiet AGN (dotted). Results are shown for 4 different ranges in velocity dispersion σ.

4.3 Emission line properties

In this section, we investigate whether there are any detectable differences in the ionization state of the narrow-line regions of the galaxies in EL-RAGN and the matched radio-quiet samples. In order to do this, we impose one further matching constraint on the radio quiet sample: we require that the value of extinction corrected [OIII] luminosities match to better than 0.15 dex.

Our results are illustrated in Figure 12. In the left-hand panel, we plot the 4000 Å break index as a function of the normalized [OIII] line luminosity L[OIII]/M_{BH}. This probes the correlation between star formation and accretion rate onto the black hole. EL-RAGN are plotted in red and the radio-quiet matches are plotted in blue. In the middle and right-hand panels, we compare the positions of both kinds of galaxies on two of the standard line diagnostic (BPT) diagrams. Results are shown in three different ranges of radio luminosity.

Figure 12 shows that to first order, EL-RAGN and their radio quiet counterparts are remarkably similar in terms of their emission line properties. There are some small differences, which are quantified in detail in Figure 13. In the left panel, we plot the distribution of $D_n(4000)$ values for the EL-RAGN with radio luminosities in excess of 3×10^{23} W Hz^{-1} in red, and the distribution of $D_n(4000)$ for their radio-quiet counterparts in blue. As can be seen, the EL-RAGN are shifted to somewhat higher values of $D_n(4000)$ Recall that the red and blue samples are exactly matched in L[OIII], so this result implies that radio-loud objects have slightly older stellar populations at a fixed value of L[OIII].

In Kauffmann et al (2003b), we introduced two parameters for characterizing the position of an AGN in the BPT diagram: a) a distance parameter D, which measures how far away the galaxy is from the star-forming locus, b) an angle parameter Φ, which characterizes the ionization state of the galaxy (i.e. the boost in [OIII]/Hβ relative to [NII]/Hα.) The middle and right panels of Figure 13 compare the distributions of D and Φ for our two samples. We find that EL-RAGN have somewhat larger values of D, but essentially identical values of Φ when compared to the radio quiet control galaxies. This is again consistent with the notion that the radio-loud AGN have slightly older stellar populations on average.

4.4 Section Summary

Overall, we find a remarkable similarity between the radio-loud and the matched radio-quiet objects in terms of host galaxy structure, stellar populations and emission line properties. Radio-loud AGN with emission lines appear to be more bulge-dominated and to have older stellar populations than their radio quiet counterparts, but the differences are very small. The most striking difference between the two types of AGN is in the environments in which they are located. We find a factor of two difference in local density between the two populations. Interestingly, this difference in environment only shows up when radio-loud AGN are compared with radio-quiet AGN. There is no correlation between the *radio luminosities* of the galaxies in the EL-RAGN sample and their environment. Best et al (2007) found a similar result for radio AGN in groups and clusters. The probability for a galaxy to be radio loud was higher in the central group/cluster galaxy when compared to other galaxies of the same stellar mass, but the distribution of radio luminosities did not depend on location within the cluster. This is somewhat puzzling, because simple jet models predict that radio galaxies should be more luminous in denser media, because adiabatic expansion losses are reduced and more energy is radiated (e.g. Kaiser, Dennett-Thorpe & Alexander 1997).

The result that radio-loud AGN with emission lines reside in denser environments than radio-quiet emission line AGN is in good agreement with the conclusions presented by Smith & Heckman (1990). It also agrees with conclusions about differences in the environments of radio-loud and radio-

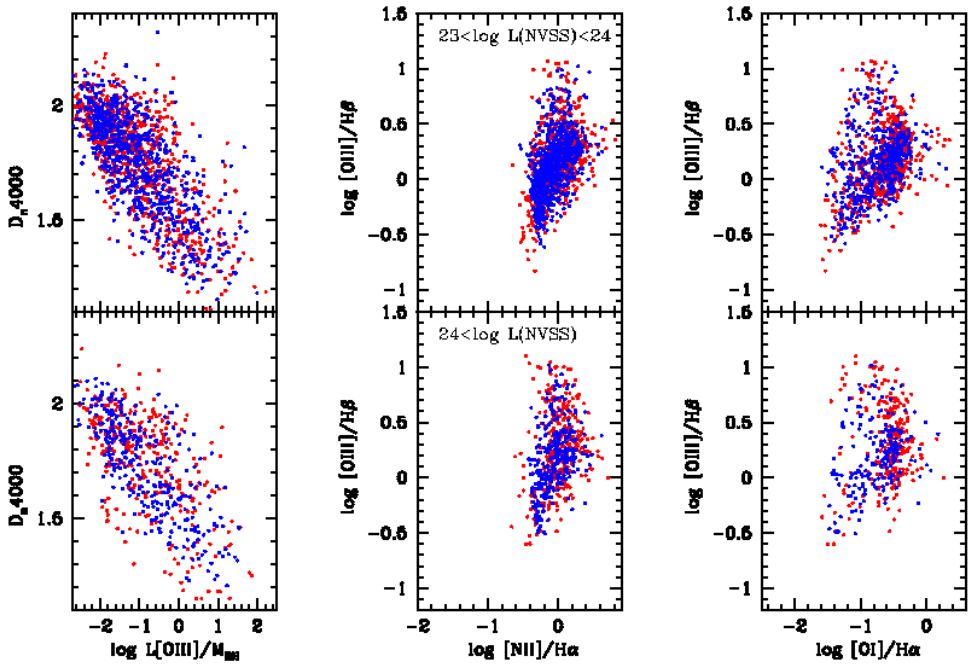

Figure 12: Comparison of emission line properties for EL-RAGN (red) and their radio quiet counterparts (blue). The left panels show the distribution of 4000 Å break strength as a function of normalized [OIII] line luminosity. The two right panels show two different examples of BPT (Baldwin, Phillips & Terlevich 1981) diagrams.

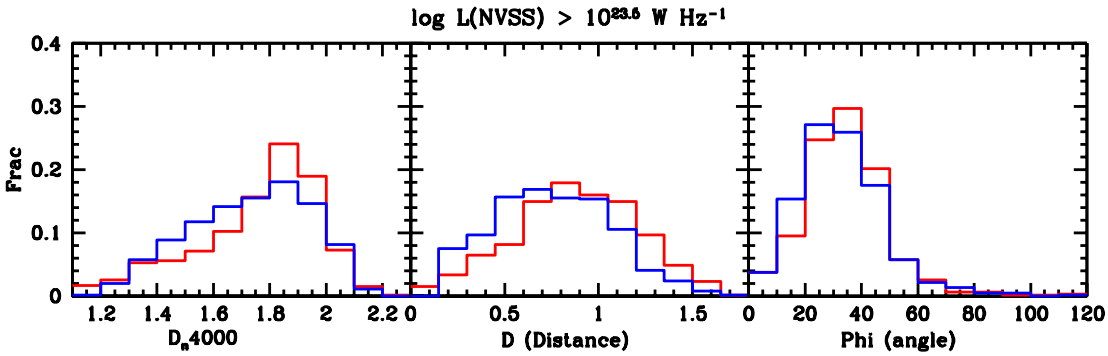

Figure 13: Quantitative comparison of emission line properties for EL-RAGN (red histogram) and their radio quiet counterparts (blue histogram). We plot distributions of 4000 Å break strength, as well as the parameters D and Φ, which quantify the location of the galaxy in the [OIII]/Hβ versus [NII]/Hα BPT diagram (see text).

quiet quasars by Yee & Green (1984) and Ellingson et al (1991), but does not agree with later work by McLure & Dunlop (2001) on this topic.

5 Which processes trigger the optical and radio AGN phenomena?

The results presented in the previous section suggest that a high density environment is required in order to produce a radio jet that is sufficiently luminous to be included in our catalogue. On the other hand, analyses of optically-selected AGN suggest that AGN with strong emission lines are almost always associated with ongoing star formation in the galaxy and, by extension, a reservoir of cold gas. Putting these two results together, *we postulate that radio-loud AGN with emission lines occur in the small subset of galaxies that contain sufficient cold gas to power strong emission lines, but also reside in high density environments.*

In the local Universe, low mass galaxies are generally gas-rich and actively star-forming, while the highest mass galaxies are almost always gas-poor and have very little ongoing star formation. This is probably why optical AGN with the highest values of $L/L_{Eddington}$ tend to occur in galaxies with the smallest bulges and black holes (Heckman et al 2004). The majority of such galaxies are found in low density environments, which are not conducive to the formation of radio-emitting jets. The requirement of high local density pushes the EL-RAGN into the peculiar parameter space of galaxies with relatively low masses that are in denser-than-average environments.

These arguments can be made more concrete by considering radio and strong emission line AGN separately and asking how they compare to matched samples of galaxies that are selected without regard to their AGN properties. Once again we choose to match in redshift, stellar mass and velocity dispersion. The radio AGN sample consists of all 5714 sources in the DR4 area with NVSS fluxes greater than 2.5 mJy that are classified as an AGN rather than star-forming (see section 2). The optical AGN sample includes 4680 objects that are selected to have log L[OIII]/$M_{BH} > 1$. This cut selects approximately 5% of all the AGN in our sample with the most rapidly growing black holes. According to the calibration between [OIII] line luminosity and accretion rate given in Heckman et al (2004), and taking into account the average extinction correction that we apply to the [OIII] line in this analysis, the black holes in these galaxies are accreting at approximately a tenth of Eddington or more.

Figure 14 compares the distributions of 4000 Å break strength and concentration index for radio AGN (red histograms) with matched samples of galaxies selected without regard to AGN properties (black). Results are shown for four different ranges of central velocity dispersion σ.

We see that the largest differences arise for the low velocity dispersion systems. Radio-loud AGN with low values of σ are shifted to higher values of both $D_n(4000)$ and concentration index compared to their matched galaxies. At the largest velocity dispersions, the distributions are almost identical. This is not surprising, because the fraction of galaxies that are radio loud approached values close to unity at the very highest masses and velocity dispersions (Best et al 2005).

Figure 15 compares the distributions of 4000 Å break strength and concentration index for our sample of powerful optical AGN (blue histograms) with matched samples galaxies selected without regard to AGN properties (black). It is clear that the trends are quite different to what is seen for the radio AGN. Strong differences arise at all velocity dispersions, but only in the properties of the stellar populations of the optical AGN, not in their structural properties. We note that these results are fully in accord with the work of Kauffmann et al (2003b), who concluded that powerful optical AGN reside in galaxies that are structurally similar to ordinary early-type systems, but have stellar populations that are considerably younger.

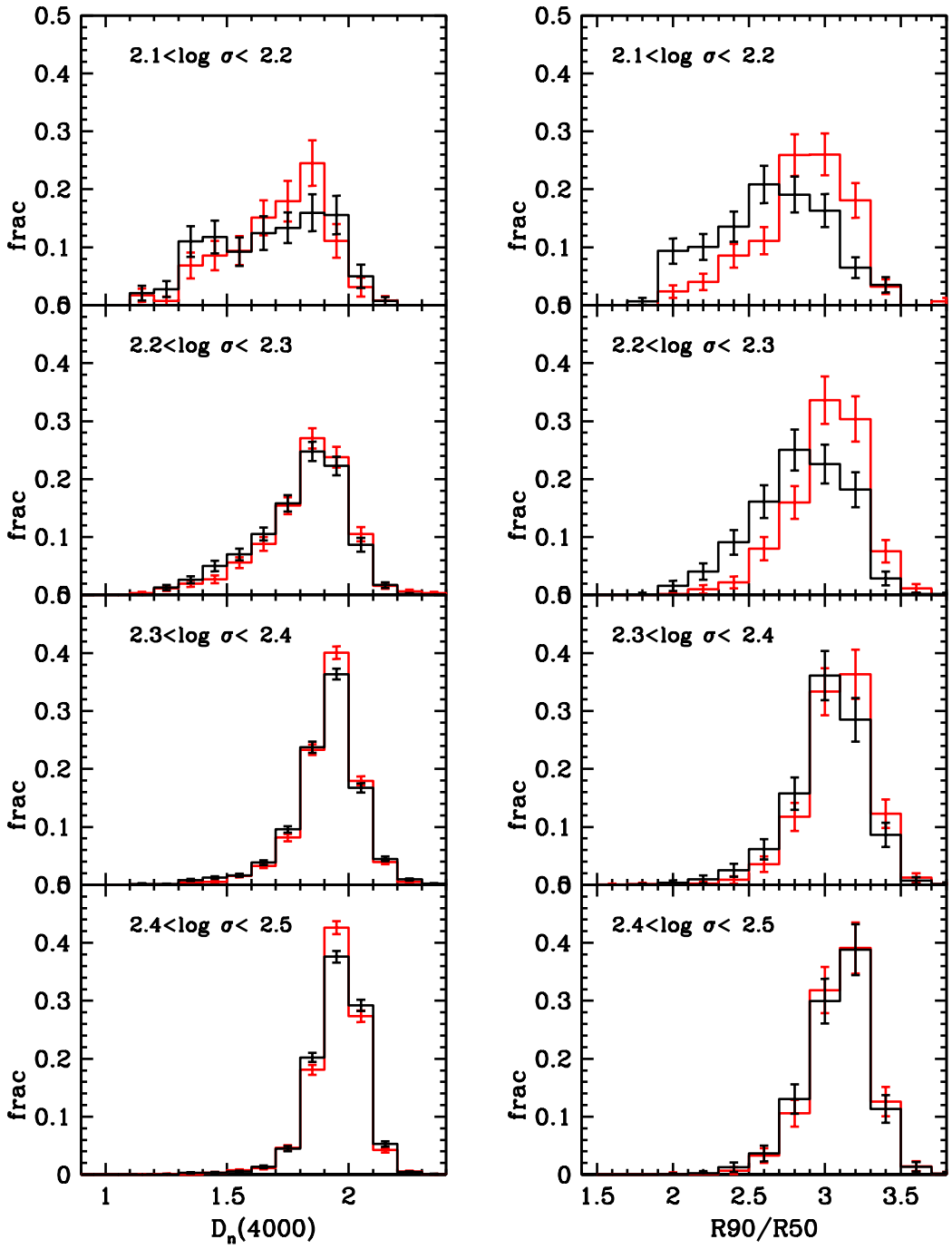

Figure 14: Comparison of the $D_n(4000)$ and concentration index distributions of our sample of radio-loud AGN (red) and a matched sample of galaxies selected without regard to AGN properties (black).

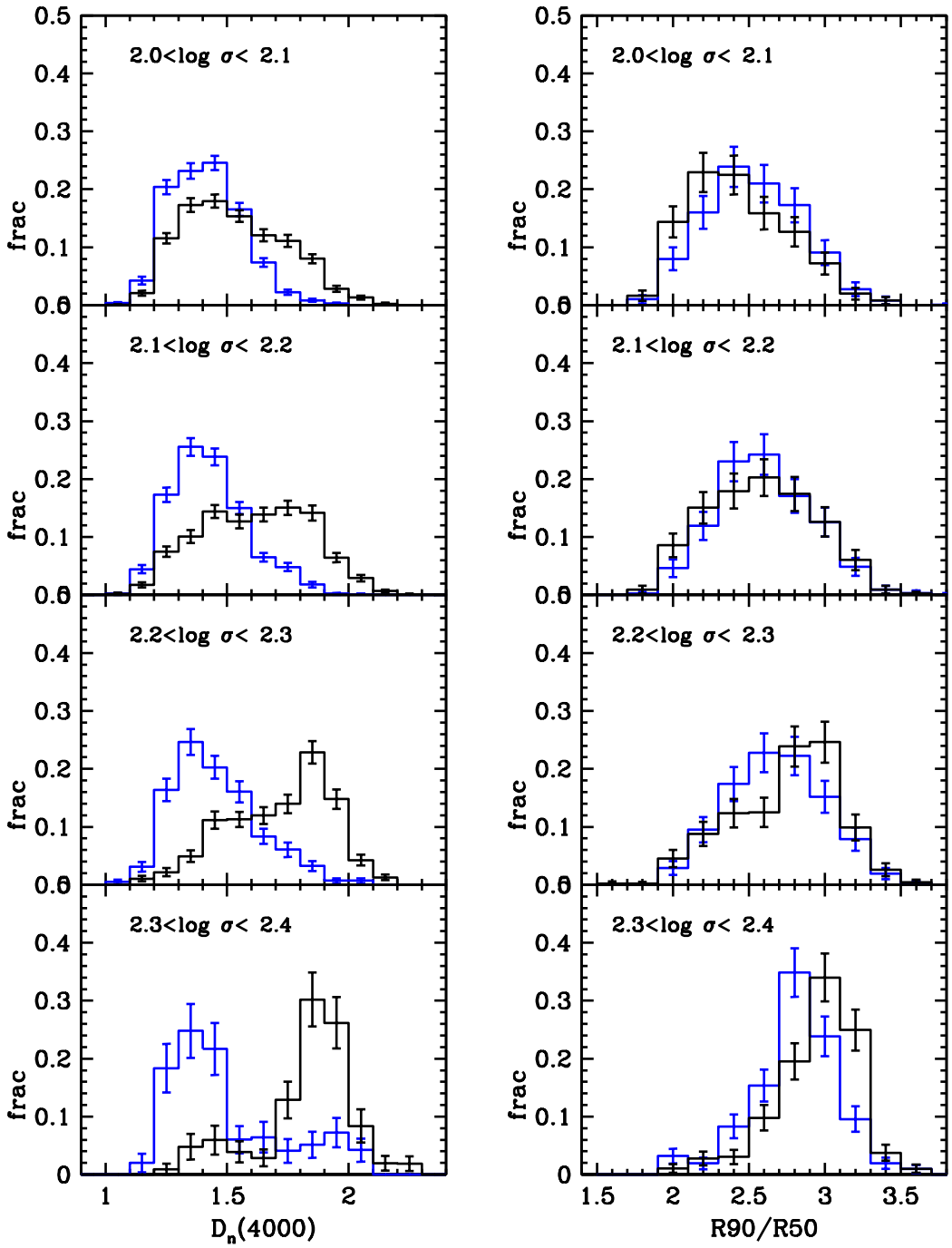

Figure 15: Comparison of the $D_n(4000)$ and concentration index distributions of our sample of our sample of powerful optical AGN with high $L[OIII]/M_{BH}$ (blue) and a matched sample of galaxies selected without regard to AGN properties (black).

We now compare the environments of the two classes of AGN with matched control samples of galaxies that are selected without regard to their AGN properties. The top panel of Figure 16 shows that radio AGN are located in denser environments than the control galaxies. Once again the differences are substantially larger for the lower velocity dispersion systems. In contrast, powerful optical AGN are always located in similar or slighty less dense environments that the control galaxies. The result on optical AGN is in agreement with the analysis of the clustering of optical AGN presented in Li et al (2006). The trends found for radio AGN agree with the results presented in Best et al (2007), who analyzed central group and cluster galaxies and found that they have a higher probability of being radio loud than other galaxies of the same stellar mass.

The figures discussed above make it clear that the conditions that are necessary for triggering a radio AGN are quite different to those necessary for triggering an optical AGN. The optical AGN phenomenon requires that the galaxy have a younger stellar population. The presence of a young stellar population is presumably linked with a supply of cold gas in the galaxy that serves as fuel for ongoing star formation and also feeds the black hole. Powerful optical AGN have very similar structural properties when compared to typical galaxies of the same velocity dispersion and mass. In contrast, the radio AGN phenomenon is not linked to the presence of young stars and cold gas in the galaxy. Radio AGN are triggered in dense environments. This is consistent with the idea that radio AGN are triggered by *hot* rather than cold gas accretion.

What happens when optical and radio AGN occur together, as is the case for the majority of powerful radio galaxies at high redshifts? Are the radio and optical modes independent or are they able to couple in some way? The fact that radio and optical line luminosities are strongly correlated in high redshift radio galaxies would suggest that the two modes are indeed coupled. In our local sample of radio AGN with emission lines, a correlation between emission line and radio luminosity also appears to be present, but it extends over a much smaller range in luminosity compared to the higher redshift radio galaxies.

Another way to look for coupling between the radio and optical phenomena is by using the matched sample technique. The bottom right panel of Figure 9 shows that when radio galaxies with emission lines are matched to a sample of radio-quiet emission line AGN, the distribution of normalized accretion rate (i.e. $L[OIII]/M_{BH}$) is identical for the two samples. This demonstrates that the presence of the radio jet does not influence the optical line emission from the AGN.

We now turn the analysis around and ask whether the presence of a strong optical AGN has any influence on the radio properties of the host galaxy. To do this, we compare the radio luminosities of the sample of powerful AGN described above with a matched sample of galaxies selected without regard to their AGN properties. In order to account for the fact that powerful optical AGN have younger stellar populations and more ongoing star formation, the control sample is matched in 4000 Å break strength in addition to redshift, stellar mass and velocity dispersion. Our results are shown in Figure 17. We plot the fraction of galaxies in the two samples as a function of radio luminosity. The first bin includes galaxies that were not detected in the radio down to a flux limit of 2.5 mJy (91.6% of the galaxies in our sample of strong optical AGN [4] versus 96.7% of the galaxies in our set of 10 control samples). Note that we plot the luminosities of *all* galaxies with radio detections independent of whether they are classified as star-forming or radio AGN. As can be seen, strong optical AGN have an enhanced probability of being detected in the radio. The enhanced detection rates persist out to radio luminosities in excess of 10^{24} W Hz^{-1}, where there are no longer any galaxies in which the radio emission can be attributed to star formation (see Fig. 1). We thus conclude that the radio and optical phenomena are not independent.

[4]It is interesting that the fraction of nearby strong optical AGN that are radio-loud is very close to the value of

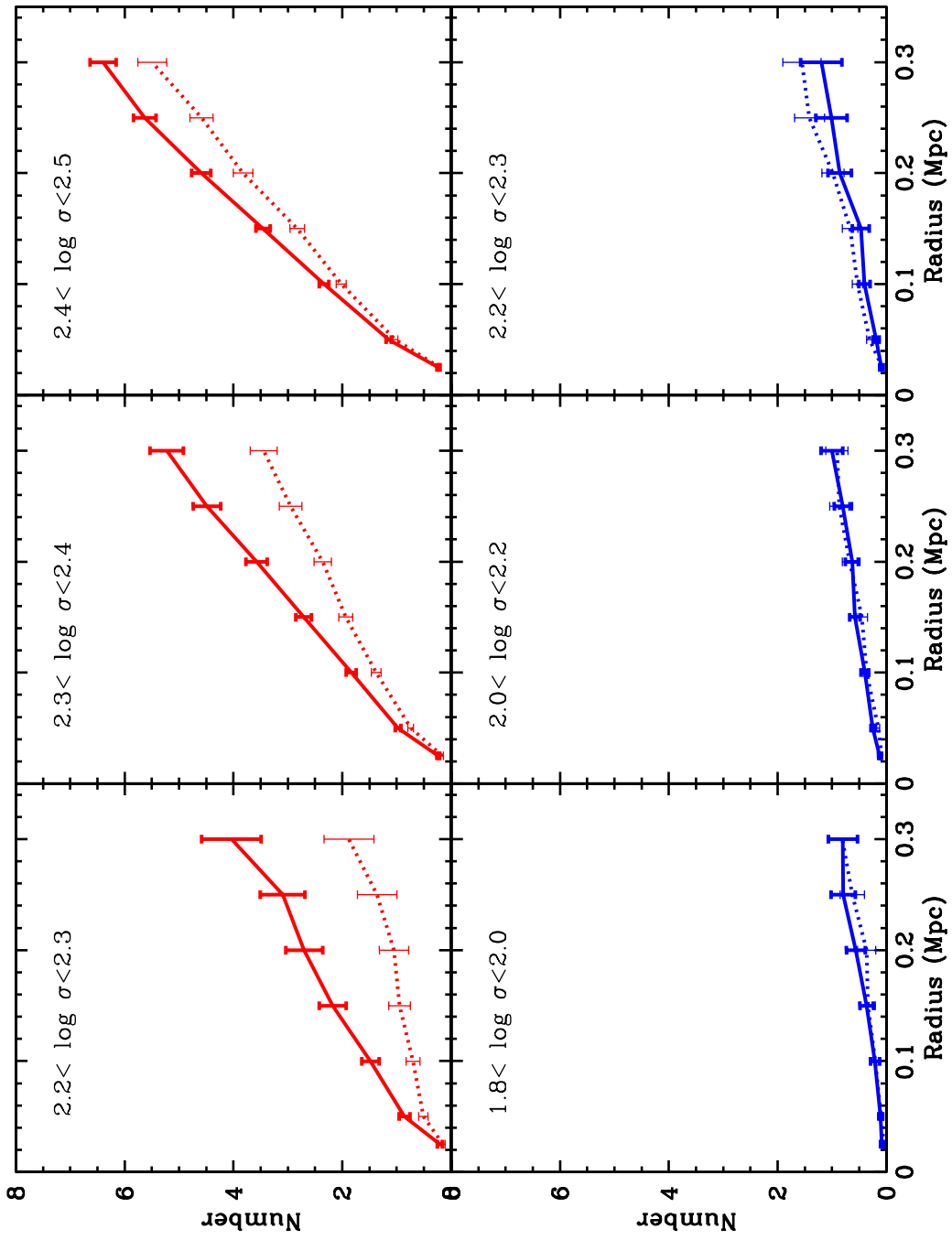

Figure 16: Comparison of the local environments of radio AGN (upper panels) and powerful optical AGN (lower panels) with matched samples of galaxies selected without regard to their AGN properties (plotted as dotted lines). We plot the average background-corrected neighbour counts interior to a given radius.

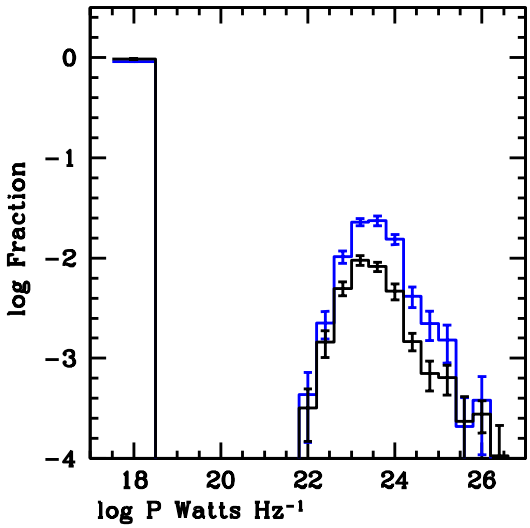

Figure 17: The distribution of radio luminosities for the sample of strong optical AGN (blue) and the matched samples of galaxies selected without regard to AGN properties (black). Note that for this plot, the control samples are matched in 4000 Å break strength in addition to redshift, stellar mass and stellar velocity dispersion.

6 Is there evidence that feedback from radio jets is responsible for regulating the star formation histories of galaxies?

In clusters, there is considerable evidence that radio AGN are able to impart considerable energy to the intra-cluster gas. This may solve the so-called "cooling flow crisis" and explain why central cluster galaxies have predominantly old stellar populations and very little ongoing star formation. Best et al (2005b,2006,2007) have argued that the same processes may be responsible for regulating the cooling of gas onto the massive galaxy population as a whole.

In principle, the matched sample technique should allow us to investigate whether the star formation histories of radio-loud AGN are any different from radio-quiet galaxies. However, in the previous sections we have seen that radio-loud AGN are located in denser regions of the Universe than their control galaxies. It is well known that there is a strong correlation between star formation in a galaxy and its local environment (e.g. Dressler 1980; Balogh et al 1999). In order to deconvolve the effect of environment and the effect of the radio jet, it is therefore necessary to compare radio-loud AGN galaxies and control galaxies at a fixed value of the local overdensity parameter.

The results of this exercise are shown in Figure 18. We use the galaxy counts within a physical radius $R < 250$ kpc as our local overdensity parameter. In order to stack galaxies at different redshifts, we do not count galaxies to a fixed limiting apparent magnitude, but to a magnitude limit of $m_r + 2.5$ mag, where m_r is the r-band magnitude of the primary galaxy. We plot $D_n(4000)$ as a function of σ for two different density regimes. Results for radio loud AGN are plotted in red and

8%±1% found for SDSS quasars by Ivezić et al (2002)

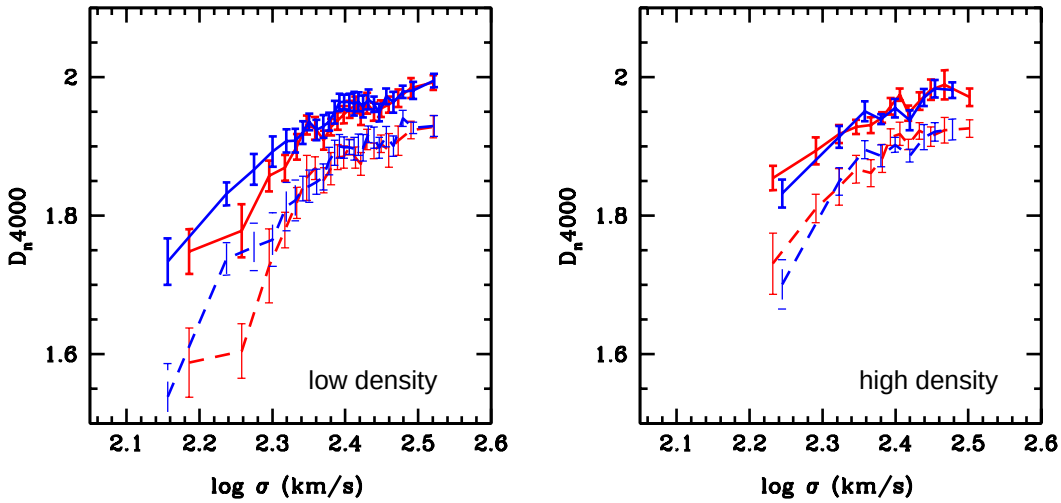

Figure 18: The relation between $D_n(4000)$ and velocity dispersion for radio-loud AGN (red) and a matched sample of galaxies selected without regard to their AGN properties (blue). Results are shown for low density environments (left) and for high density environments (right). The solid line indicates the median value of $D_n(4000)$ at a given value of σ, while the dashed line indicates the lower 25th percentile of the distribution.

results for radio-quiet matched galaxies are shown in blue. The solid line indicates the median value of $D_n(4000)$ at a given value of σ, while the dashed line indicates the lower 25th percentile of the distribution. For massive galaxies with large values of σ, there is no discernible difference between the two samples. This holds both in high density and in low density regions. For less massive galaxies in lower density regions, radio loud AGN are shifted to slightly lower values of $D_n(4000)$ compared to the control galaxies.

The fact that there is very little difference between the stellar populations of radio-loud and radio-quiet massive galaxies means that the interplay between heating, cooling, and star formation must be in a finely-balanced, self-regulated state. B05b show that the radio-loud duty-cycle is large in the most massive galaxies, implying that the radio jet is heating the surrounding gas more or less continuously. We speculate that in low mass galaxies that reside in lower mass halos, heating,cooling and star formation may not be as finely balanced. The duty cycle of the radio-loud phase is much smaller, so the radio source must have a longer-lasting effect. Galaxies with small values of the local density parameter are typically located in less massive dark matter halos than galaxies with large values of this parameter (see Kauffmann et al 2004). The fact that the radio loud AGN in low density environments have slightly younger stellar populations may indicate that the radio jet switches on at the time when gas cooling/accretion and its associated star formation are at a peak in these systems. In a recent paper, Croston, Kraft & Hardcastle (2007) have analyzed shock-heated shells of hot gas surrounding a nearby radio galaxy. Their estimate of the amount of energy stored in these shells shows that shock-heating during the early super-sonic expansion phase can have lasting effects on the interstellar medium of the host galaxy.

7 Summary and Discussion

In the local Universe, the majority of radio-loud AGN are found in massive elliptical galaxies with weak or absent emission lines and very little ongoing star formation. Because these galaxies contain very little cold gas, the radio jet has been hypothesized to be powered by accretion from a halo of pressure-supported hot gas that surrounds these galaxies (e.g. Allen et al 2006). Thermal bremsstrahlung from this gas is often detectable if sufficiently deep X-ray observations are available. In the high redshift Universe, radio galaxies are very different. Almost all powerful high redshift radio galaxies have strong emission lines, and there is ample evidence that the host galaxies of these systems are often disturbed and are experiencing a significant level of ongoing star formation (e.g. Best et al 1998; Pentericci et al 2003; Zirm et al 2003). It is thus reasonable to suppose that accretion of cold gas may play an important role in these galaxies.

Our paper focuses on a subset of radio AGN selected from the Sloan Digital Sky Survey that do have emission lines. We explore the hypothesis that these objects are local analogs of powerful high-redshift radio galaxies and we ask how they differ from their nearby radio-quiet counterparts.

In the local Universe, the probability for a radio AGN to have emission lines is a strongly decreasing function of galaxy mass or velocity dispersion. The frequency of radio AGN with emission lines also rises strongly at radio luminosities greater than 10^{25} W Hz^{-1}. We show that the emission line and radio luminosities are correlated in these objects, but with substantial scatter. Interestingly, a significiant component of the scatter can be directly attributed to the velocity dispersion/black hole mass of the host galaxy: to reach a given radio power (i.e. a given rate of mechanical energy carried by the jet), smaller black holes require higher [OIII] luminosities (which we interpret as higher accretion rates) than bigger black holes. However, if we scale the emission line and radio luminosities by dividing by σ^4 (i.e. by the black hole mass), we find that our sample of RL-AGN define a correlation between normalized radio power and accretion rate in Eddington units that is independent of black hole mass. At the present day, EL-RAGN with high values of $\log P/M_{BH}$ reside in galaxies with smaller mass black holes than EL-RAGN with low values of $\log P/M_{BH}$.

Our results lead to a very simple explanation for why very powerful emission line radio galaxies are much more common at high redshifts. In the local Universe, as a result of a process that has been dubbed "down-sizing", only low mass black holes are actively growing and accreting at rates close to Eddington at the present day. As we have shown, the radio jets produced by these systems are relatively weak. At high redshifts, massive black holes are growing and these obejcts will produce much more powerful jets. Our data provide some degree of quantitative support for this scenario – we show that the relation between emission line and radio luminosity derived for powerful high redshift radio galaxies matches the correlation that we measure for our sample of low-redshift radio galaxies with large black hole masses and also extends it to higher radio power.

In the second part of the paper, we investigate the question of *why* only a small fraction of emission line AGN become radio loud. We do this by creating matched samples of radio-loud and radio-quiet AGN and asking whether we can find any systematic differences in their host galaxy properties and environments. We find that the main difference between radio-loud and radio-quiet AGN lies in their environments; radio-loud AGN are found in regions with local density estimates that are larger by a factor of 2-3. The most plausible explanation of this result is that the production of luminous radio jets is strongly favoured by the presence of a quasi-static, pressure-supported halo of hot gas. With our current set of observational data, we are not able to tell whether a hydrostatic halo is required in order to *form* the jet in the first place, or whether the halo is merely required in order dissipate its energy (i.e. the hot gas halo is merely a working surface for the jet). Higher resolution radio data (e.g. Gallimore et al 2006) may help distinguish between these two scenarios.

We note that the fact that the radio luminosity of the jet and the strength of the emission lines are correlated in radio galaxies with emission lines, means that the cold gas and hot gas phases are not decoupled. Our matched sample experiments show that strong optical AGN have a significantly enhanced probability of hosting radio jets. We also find that *all* radio AGN with radio luminosity per unit black hole mass of 10^{17} W Hz^{-1} $M_{\odot}^{-1}$ exhibit strong emission lines and evidence of recent star formation, which strongly suggests that the cold ISM must play a role in determining the jet power in these objects.

The difference between the "formation" and the "working surface" hypotheses is important for understanding how jets are generated by the black hole, but less important for understanding the impact of radio AGN on galaxy evolution. This will mainly depend on how the interplay between cold and hot gas accretion evolves as a function of redshift. As has been extensively discussed in a number of recent papers (Birnboim & Dekel 2003; Keres et al 2005; Croton et al 2006), the transition between the accretion of cold gas along filaments and the accretion of hot gas from a quasi-static, pressure-supported halo always occurs at a dark matter halo mass of $\sim 10^{12} M_{\odot}$. If optical AGN are fuelled primarily by cold gas accretion and radio AGN by hot gas accretion, we would expect radio AGN to be located in significantly more massive halos than optical AGN at all redshifts. Our local density estimator, which counts the number of neighbours within a few hundred kiloparsecs of the galaxy, is expected to scale quite closely with the mass of the surrounding halo (Kauffmann et al 2004). In future work, we will explore whether our observational results are in quantitative agreement with a model in which radio galaxies only reside in halos greater than this minimum mass.

In this scenario, radio-loud AGN with strong emission lines occupy a restricted region of parameter space; we would expect them to be located in environments where both cold and hot gas accretion can occur *simultaneously*. In the low redshift Universe, cold gas is only present in low mass galaxies that are usually located in low mass halos. The majority of massive galaxies have very little cold gas and a large fraction are located in halos considerably more massive than the transition mass of $10^{12} M_{\odot}$. This explains why radio galaxies with emission lines are rare in our low redshift sample and why they are restricted to galaxies with low values of σ located in denser-than-average environments. At high redshifts, however, the situation will be quite different. Massive galaxies will be located in considerably smaller halos and they may well still be accreting cold gas and thus be capable of hosting powerful radio AGN with emission lines. This will be the subject of future work.

Finally, we have explored whether radio-loud AGN have systematically different star formation histories compared to matched samples of radio-quiet galaxies. This comparison is interesting, because it sheds light on the manner in which radio jets regulate the growth of galaxies through star formation. Because star formation rate and local galaxy density are known to be correlated, and because radio AGN are found in denser-than-average regions of the Universe, we carry out our comparison between radio-loud and radio-quiet objects at a fixed local density.

In the most massive galaxies and in the densest environments, the duty cycle of the radio AGN phenomenon is very high (B05b show that the fraction of radio AGN reaches values close to 50% for the most massive galaxies on the local Universe). It is perhaps not too surprising, therefore, that for these systems the age of the stellar population does not depend on whether the galaxy is radio-loud or radio-quiet. The radio jet is heating the gas more or less continuously and star formation rates are maintained at very low levels. It is only for low mass galaxies located in low-density environments (i.e. in low mass halos) that significant differences between the radio-loud AGN and control samples of normal galaxies begin to emerge. We find that in these systems radio jets are preferentially located in galaxies with systematically younger stellar populations. This means that in low mass halos, the radio jet is dumping its energy in the vicinity of those objects that are currently experiencing higher-than-average rates of star formation (see Figure 18).

In the local Universe, radio AGN in young, star-bursting galaxies are rare and are not intrinsically very powerful because they are powered by relatively low mass black holes. However, at higher redshifts massive black holes are alive and awake and the effects of the much more powerful radio jet may be considerably more dramatic (Nesvadba et al 2006). As more and more data on high redshift galaxies is accumulated, it should become increasingly possible to apply the lessons learned from studying galaxies and AGN at low redshifts in order to figure out which physical processes dominate as a function of cosmic epoch.

Acknowledgements

We thank Roderik Overzier for stimulating, useful and amusing discussions.
Funding for the creation and distribution of the SDSS Archive has been provided by the Alfred P. Sloan Foundation, the Participating Institutions, the National Aeronautics and Space Administration, the National Science Foundation, the U.S. Department of Energy, the Japanese Monbukagakusho, and the Max Planck Society. The SDSS Web site is http://www.sdss.org/. The SDSS is managed by the Astrophysical Research Consortium (ARC) for the Participating Institutions. The Participating Institutions are The University of Chicago, Fermilab, the Institute for Advanced Study, the Japan Participation Group, The Johns Hopkins University, the Korean Scientist Group, Los Alamos National Laboratory, the Max-Planck-Institute for Astronomy (MPIA), the Max-Planck-Institute for Astrophysics (MPA), New Mexico State University, University of Pittsburgh, University of Portsmouth, Princeton University, the United States Naval Observatory, and the University of Washington.

References

Allen S. W., Dunn R. J. H., Fabian A. C., Taylor G. B., Reynolds C. S., 2006, MNRAS, 372, 21

Baldwin J. A., Phillips M. M., Terlevich R., 1981, PASP, 93, 5 (BPT)

Balogh M. L., Morris S. L., Yee H. K. C., Carlberg R. G., Ellingson E., 1999, ApJ, 527, 54

Barthel, P. D., 1989, ApJ, 336, 606

Baum S. A., Zirbel E. L., O'Dea C. P., 1995, ApJ, 451, 88

Becker R. H., White R. L., Helfand D. J., 1995, ApJ, 450, 559

Best, P. N., Longair, M. S., & Röttgering, H. J. A., 1998, MNRAS, 295, 549

Best P. N., Kauffmann G., Heckman T. M., Brinchmann J., Charlot S., Ivezić Ž., White S. D. M., 2005a, MNRAS, 362, 25 (B05a)

Best P. N., Kauffmann G., Heckman T. M., Ivezić Ž., 2005b, MNRAS, 362, 9 (B05b)

Best P. N., Kaiser C. R., Heckman T. M., Kauffmann G., 2006, MNRAS, 368, L67

Best P. N., von der Linden A., Kauffmann G., Heckman T. M., Kaiser C. R., 2007, MNRAS, in press

Birnboim Y., Dekel A., 2003, MNRAS, 345, 349

Birzan L., Rafferty D. A., McNamara B. R., Wise M. W., Nulsen P. E. J., 2004, ApJ,607,800

Boehringer H., Voges W.,Fabian A. C., Edge A. C., Neumann D. M., 1993, MNRAS, 264, L25

Bower R. G., Benson A. J., Malbon R., Helly J. C., Frenk C. S., Baugh C. M., Cole S., Lacey C. G., 2006, MNRAS, 370, 645

Brinchmann J., Charlot S., White S. D. M., Tremonti C., Kauffmann G., Heckman T., Brinkmann J., 2004, MNRAS, 351, 1151

Bruzual G., Charlot S., 2003, MNRAS, 344, 1000

Charlot S., Fall S. M., 2000, ApJ, 539, 718

Churazov E., Brueggen M., Kaiser C. R., Boehringer H., Forman W., 2001, ApJ, 554, 261

Clewley L., Jarvis M. J., 2004, MNRAS, 352, 909

Condon J. J., Cotton W. D., Greisen E. W., Yin Q. F., Perley R. A., Taylor G. B., Broderick J. J., 1998, AJ, 115, 1693

Croston J. H., Kraft R. P., Hardcastle M. J., 2007, ApJ, 660, 191

Croton D. J., et al., 2006, MNRAS, 365, 11

Dressler A., 1980, ApJ, 236, 531

Dunlop J. S., Peacock J. A., 1990, MNRAS, 247, 19

Di Matteo T., Springel V., Hernquist L., 2005, Natur, 433, 604

Ellingson E., Yee H. K. C., Green R. F., 1991, ApJ, 371, 49

Fabian A. C., et al., 2000, MNRAS, 318, L65

Fabian A. C., Sanders J. S., Allen S. W., Crawford C. S., Iwasawa K., Johnstone, R. M., Schmidt R. W., Taylor G. B., 2003, MNRAS, 344, L43

Fabian A. C., Sanders J. S., Taylor G. B., Allen S. W., 2005, MNRAS, 360, L20

Fanaroff B. L., Riley J. M., 1974, MNRAS, 167, 31P

Forman, W., et al., 2005, ApJ, 635, 894

Gallimore J. F., Axon D. J., O'Dea C. P., Baum S. A., Pedlar A., 2006, AJ, 132, 546

Govoni F., Falomo R., Fasano G., Scarpa R., 2000, A&A, 353, 507

Hardcastle M. J., Evans D. A., Croston J. H., 2006, MNRAS, 370, 1893

Hardcastle M. J., Evans D. A., Croston J. H., 2007, MNRAS, 376, 1849

Heckman T. M., Kauffmann G., Brinchmann J., Charlot S., Tremonti C., White S. D. M., 2004, ApJ, 613, 109

Hine R. G., Longair M. S., 1979, MNRAS, 188, 111

Hopkins P. F., Hernquist L., Cox, T.J., Di Matteo T., Martini P., Robertson, B., Springel, V., 2005, ApJ, 630, 705

Ivezić Ž., et al., 2002, AJ, 124, 2364

Kaiser C. R., Dennett-Thorpe J., Alexander P., 1997, MNRAS, 292, 723

Kauffmann G., et al., 2003a, MNRAS, 341, 33

Kauffmann G., et al., 2003b, MNRAS, 346, 1055

Kauffmann G., White S. D. M., Heckman T. M., Ménard B., Brinchmann J., Charlot S., Tremonti C., Brinkmann J., 2004, MNRAS, 353, 713

Kereš D., Katz N., Weinberg D. H., Davé R., 2005, MNRAS, 363, 2

Laing R. A., Riley J. M., Longair M. S., 1983, MNRAS, 204, 151

Laing R. A., Jenkins C. R., Wall J. V., Unger S. W., 1994, ASPC, 54, 201

Ledlow M. J., Owen F. N., 1995, AJ, 109, 853

Li C., Kauffmann G., Wang L., White S. D. M., Heckman T. M., Jing Y. P., 2006, MNRAS, 373, 457

McCarthy P. J., 1993, ARA&A, 31, 639

McLure, R. J., Dunlop, J. S., 2001, MNRAS, 321, 515

Nesvadba N. P. H., et al., 2006, ApJ, 650 639,

Pentericci, L., Röttgering, H. J. A., Miley, G. K., McCarthy, P., Spinrad, H., van Breugel, W. J. M., & Macchetto, F.,1999, A&A , 341, 329

Sijacki D., Springel V., Di Matteo T., Hernquist L., 2007, arXiv, 705, arXiv:0705.2238

Smith E. P., Heckman T. M., 1989, ApJ, 341, 658

Tadhunter C., Dickson R., Morganti R., Robinson T. G., Wills K., Villar-Martin M., Hughes M., 2002, MNRAS, 330, 977

Tadhunter C., Robinson T. G., González Delgado R. M., Wills K., Morganti R., 2005, MNRAS, 356, 480

Tremaine S., et al., 2002, ApJ, 574, 740

Tremonti C. A., et al., 2004, ApJ, 613, 898

Wild V., Kauffmann G., Heckman T., Charlot S., Lemson G., Brinchmann J., Reichard T., Pasquali A., 2007, arXiv, 706, arXiv:0706.3113

Worthey G., Ottaviani D. L., 1997, ApJS, 111, 377

Yee, H. K. C., Green, R. F., 1984, ApJ, 280, 79

Yun M. S., Reddy N. A., Condon J. J., 2001, ApJ, 554, 803

Zirbel E. L., Baum S. A., 1995, ApJ, 448, 521 (ZB)

Zirm, A. W., Dickinson, M., & Dey, A., 2003, ApJ, 585, 90